*inorganics*

MDPI

*Article*

# Synthesis, Characterization, DNA Binding and Cytotoxicity of Copper(II) Phenylcarboxylate Complexes

**Carlos Y. Fernández [1,2], Analu Rocha [3], Mohammad Azam [4], Natalia Alvarez [1], Kim Min [5], Alzir A. Batista [3], Antonio J. Costa-Filho [6], Javier Ellena [7] and Gianella Facchin [1,*]**

1 Química Inorgánica, Departamento Estrella Campos, Facultad de Química, Universidad de la República, Montevideo 11800, Uruguay; cyanez@fq.edu.uy (C.Y.F.)
2 Programa de Posgrados de la Facultad de Química, Facultad de Química, Universidad de la República, Gral. Flores 2124, Montevideo 11800, Uruguay
3 Departamento de Química, Federal University of São Carlos, CP 676, São Carlos 13565-905, SP, Brazil
4 Department of Chemistry, College of Sciences, King Saud University, P.O. Box 2455, Riyadh 11451, Saudi Arabia
5 Department of Safety Engineering, Dongguk University, 123 Dongdae-ro, Gyeongju 780714, Gyeongbuk, Republic of Korea
6 Physics Department, Ribeirão Preto School of Philosophy, Science and Literature, University of São Paulo, Av. Bandeirantes, Ribeirão Preto 14040-901, SP, Brazil
7 São Carlos Institute of Physics, University of São Paulo, Av. do Trabalhador São-Carlense 400, São Carlos 13566-590, SP, Brazil
* Correspondence: gfacchin@fq.edu.uy

**Abstract:** Coordination compounds of copper exhibit cytotoxic activity and are suitable for the search for novel drug candidates for cancer treatment. In this work, we synthesized three copper(II) carboxylate complexes, $[Cu_2(3\text{-}(4\text{-hydroxyphenyl})propanoate)_4(H_2O)_2]\cdot 2H_2O$ (**C1**), $[Cu_2(phenylpropanoate)_4(H_2O)_2]$ (**C2**) and $[Cu_2(phenylacetate)_4]$ (**C3**), and characterized them by elemental analysis and spectroscopic methods. Single-crystal X-ray diffraction of **C1** showed the dinuclear paddle-wheel arrangement typical of Cu–carboxylate complexes in the crystal structure. In an aqueous solution, the complexes remain as dimeric units, as studied by UV-visible spectroscopy. The lipophilicity (partition coefficient) and the DNA binding (UV visible and viscosity) studies evidence that the complexes bind the DNA with low $K_b$ constants. In vitro cytotoxicity studies on human cancer cell lines of metastatic breast adenocarcinoma (MDA-MB-231, MCF-7), lung epithelial carcinoma (A549) and cisplatin-resistant ovarian carcinoma (A2780cis), as well as a nontumoral lung cell line (MRC-5), indicate that the complexes are cytotoxic in cisplatin-resistant cells.

**Keywords:** copper complexes; phenyl-carboxylate; DNA interaction; cytotoxic activity

check for updates

**Citation:** Fernández, C.Y.; Rocha, A.; Azam, M.; Alvarez, N.; Min, K.; Batista, A.A.; Costa-Filho, A.J.; Ellena, J.; Facchin, G. Synthesis, Characterization, DNA Binding and Cytotoxicity of Copper(II) Phenylcarboxylate Complexes. *Inorganics* **2023**, *11*, 398. https://doi.org/10.3390/inorganics11100398

Academic Editor: Vladimir Arion

Received: 4 September 2023
Revised: 5 October 2023
Accepted: 8 October 2023
Published: 11 October 2023

**Copyright:** © 2023 by the authors. Licensee MDPI, Basel, Switzerland. This article is an open access article distributed under the terms and conditions of the Creative Commons Attribution (CC BY) license (https://creativecommons.org/licenses/by/4.0/).

## 1. Introduction

Metal-based drugs play an important role in cancer treatment. Cisplatin and its congeners (carboplatin, oxalylplatin, heptaplatin and picoplatin) are successfully used against various cancer types, being curative in several cases [1]. Despite this, there is still a lack of effective treatment for all types of cancer. Furthermore, despite offering a variety of compounds and mechanisms of action, the development of new potential anticancer metallopharmaceuticals remains mainly academic, possibly due to the complexity of metal-coordination compounds' reactivity [2].

Copper-coordination compounds are an attractive class of compounds for the development of novel cancer treatments [2–5]. Different copper complexes with antitumor activity have been synthesized and characterized, with promising results, even presenting antimetastatic and antiangiogenic activities (in vitro assays) or being cytotoxic to cancer stem cells [3,4,6–13]. Cu(II) complexes of ligands with no appreciable cytotoxic activity are active, indicating that the metal itself plays a role in antitumor activity.

The mechanism of action of copper compounds may include various molecular processes, which have not been thoroughly characterized [3,4,13]. The lack of specificity against a single molecular target strengthens copper complexes' ability to fight a diverse cell population, such as those found in a tumor. DNA binding and producing reactive oxygen species (ROS), inducing redox stress, are commonly proposed as molecular events for most anticancer copper compounds [2,4,14–16].

As a part of our research of copper complexes with cytotoxic activity [17–25], we search for simple molecules, especially those already tested for their biological use, that can act as anion ligands. Phenylacetic acid is a compound used to treat high nitrogen levels in hepatic patients and, therefore, meets the safety regulations to be used as a drug [26]. In this work, we explored the chemical properties and cytotoxicity of copper complexes with phenylacetic acid, as well as two related compounds, phenylpropanoate and 3-(4-hydroxyphenyl)propanoate, in order to prepare complexes with varying lipophilicity and possibly other differences in chemical behavior.

The complexes were studied both in the solid state and aqueous solution, including a new crystal structure. The binding of the complexes to the DNA molecule was investigated. The cytotoxicity of the complexes was evaluated against MDA-MB-231, MCF-7 (human metastatic breast adenocarcinomas, the first triple negative), A549 (human lung epithelial carcinoma), A2780cis (cisplatin-resistant human ovarian carcinoma, SIGMA) and MRC-5 (human nontumoral lung epithelial cells), finding an interesting activity on cisplatin-resistant A2780cis cells.

## 2. Results

As described in the experimental section, three complexes were synthesized: $[Cu_2(3\text{-}(4\text{-hydroxyphenyl})propanoate)_4(H_2O)_2]\cdot 2H_2O$ (**C1**); $[Cu_2(phenylpropanoate)_4(H_2O)_2]$ (**C2**); and $[Cu_2(phenylacetate)_4]$ (**C3**).

### *2.1. Crystal Structures*

The obtained complexes were recrystallized from water by slow evaporation at room temperature. Single crystals suitable for X-ray diffraction analysis were obtained only for **C1**, a new compound, and **C3**, which had two previously reported [27,28]. The most relevant structural features are described in this section. Table 1 summarizes crystallographic data and refinement details. A scheme of the complexes and the ligands is included in the supplementary material (Figure S1).

**Table 1.** Crystallographic data and refinement details for **C1** and **C3**.

| Complex | C1 | C3 |
|---|---|---|
| Formula | $C_{36}H_{44}Cu_2O_{16}$ | $C_{16}H_{14}CuO_4$ |
| $D_{calc.}$/g cm$^{-3}$ | 1.594 | 1.618 |
| $\mu$/mm$^{-1}$ | 2.130 | 2.374 |
| Formula Weight | 859.832 | 333.81 |
| Color | Blue | Blue |
| Shape | Prism | Plate |
| Size/mm$^3$ | 0.15 × 0.10 × 0.10 | 0.30 × 0.15 × 0.08 |
| Crystal System | Triclinic | monoclinic |
| Space Group | $P\bar{1}$ | $P2_1/c$ |
| $a$/Å | 8.6810(2) | 5.17356(6) |
| $b$/Å | 10.6746(3) | 26.2143(3) |
| $c$/Å | 11.3849(3) | 10.20173(12) |
| $\alpha$/° | 66.930(3) | 90 |
| $\beta$/° | 70.661(2) | 97.8378(11) |
| $\gamma$/° | 71.814(2) | 90 |
| V/Å$^3$ | 895.43(5) | 1370.64(3) |
| Z | 1 | 4 |

**Table 1.** *Cont.*

| Complex | C1 | C3 |
|---|---|---|
| $\Theta_{min}$ /° | 4.347 | 3.372 |
| $\Theta_{max}$ /° | 80.066 | 79.397 |
| Measured Refl. | 15,912 | 13,429 |
| Independent Refl. | 3875 | 2965 |
| Reflections with I > 2σ(I) | 3820 | 2743 |
| $R_{int}$ | 0.0193 | 0.0451 |
| Parameters | 251 | 191 |
| Restraints | 0 | 0 |
| Largest Peak | 0.622 | 0.476 |
| Deepest Hole | −0.737 | −0.597 |
| GooF | 1.040 | 1.027 |
| $wR_2$ (all data) | 0.0708 | 0.0855 |
| $wR_2$ | 0.0706 | 0.0835 |
| $R_1$ (all data) | 0.0278 | 0.0349 |
| $R_1$ | 0.0275 | 0.0325 |
| CCDC deposition number | 2,288,430 | 2,288,436 |

#### 2.1.1. $[Cu_2(3\text{-}(4\text{-Hydroxyphenyl})propanoate)_4(H_2O)_2]\cdot 2H_2O$

$[Cu_2(3\text{-}(4\text{-hydroxyphenyl})propanoate)_4(H_2O)_2]\cdot 2H_2O$, **C1**, crystallizes in the triclinic space group $P\bar{1}$ with one molecular formula per unit cell. Figure 1 presents both the asymmetric and cell unit of the structure, whereas Table 2 indicates bond lengths (Å) and angles (°) surrounding the coordination center. The copper ion presents a pentacoordinated environment where the equatorial donors are four carboxylate O atoms from four different ligands, and the apical position is occupied by an O atom from a water molecule. The carboxylate group acts as a bridging bidentate ligand, connecting the two copper(II) centers in the dimeric molecule. Figure 1b presents the molecular moiety where the dimeric paddle-well arrangement typical of dimeric Cu–carboxylate complexes can be observed. This motif is observed on several Cu(II) compounds with ligands containing carboxylate groups, such as acetate [29,30], propionate [31], dinitrobenzoates [32] and N-acetylglycinato [33], among others.

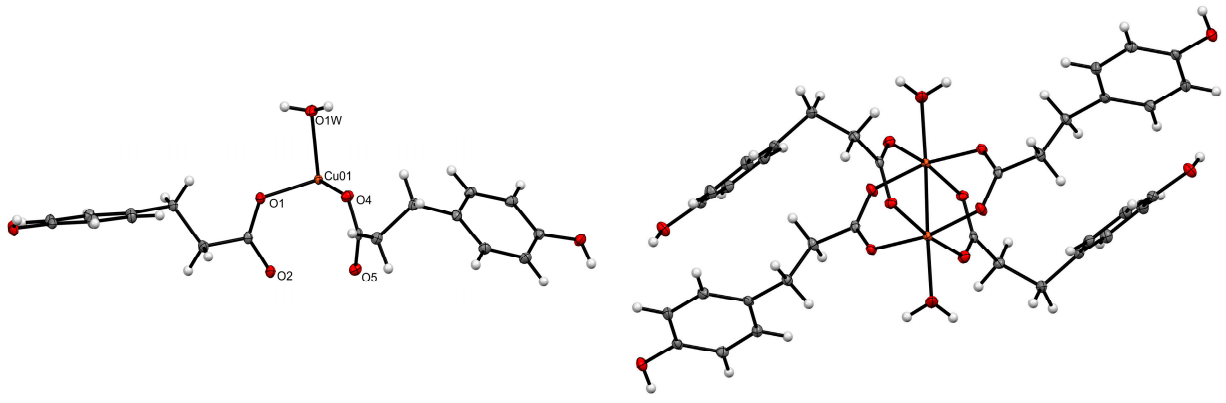


(**a**) (**b**)

**Figure 1.** ORTEP representation at 50% probability of (**a**) the asymmetric unit and (**b**) molecular moiety of $[Cu_2(3\text{-}(4\text{-hydroxyphenyl})propanoate)_4(H_2O)_2]\cdot 2H_2O$ (**C1**). The hydration water molecule is omitted for clarity. Atom color code: Cu (orange), C (gray), O (red) and H (white).

**Table 2.** Selected bond lengths (Å) and angles (°) for **C1**.

| Bond Lengths (Å) | | Angles (°) | |
|---|---|---|---|
| Cu1-Cu2 | 2.6075(4) | O1-Cu1-O4 | 90.98(5) |
| Cu1-O4 | 1.9649(11) | O5′-Cu1-O4 | 169.16(4) |
| Cu1-O1 | 1.9604(10) | O5′-Cu1-O1 | 88.48(4) |
| Cu1-O5′ | 1.9751(10) | O2′-Cu1-O4 | 91.39(5) |
| Cu1-O2′ | 1.9628(11) | O2′-Cu1-O1 | 168.36(5) |
| | | O5′-Cu1-O2′ | 87.05(5) |

A crystallographic database search in the CSD [34] v2022.3.0, conducted using Conquest [35], found 786 related structures, which were analyzed in Mercury [36]. The bridging bidentate mode of coordination of the carboxylate group determines Cu···Cu distances in this dinuclear paddle-wheel type complexes. The distances in the analyzed structures range from 2.58 to 2.68 Å, including the 2.608 Å distance observed in **C1**. Other structures containing a 2.608 Å Cu···Cu distance include structures with acetate [37], propionate [31,38], benzoate [39,40] and paranitrobenzoate [41] as ligands.

The crystal packing is sustained primarily by strong classical H-bond interactions [42] involving the hydroxyl and carboxylate groups in the ligand and the coordinated and lattice water molecules. Each hydroxyl group acts as an H-bond acceptor with a coordinated water molecule in a contiguous complex molecule (H···O distance of 1.898 Å, O-H-O angle 172.4°) and donor with a lattice water molecule (H···O distance of 1.903 Å, O-H-O angle 172.5°). The lattice water molecule also acts as an H-bond donor to a carboxylate O atom with an H···O distance of 2.028 Å and an O-H-O angle of 153.0°. Nonclassical H-bonds are also observed in the C-H···π interactions between phenyl rings of ligands in contiguous molecules with a centroid to H distance of 2.658 Å and the angle between the phenyl rings of 47.45°.

#### 2.1.2. $[Cu_2(Phenylacetate)_4]\cdot 2H_2O$ and $[Cu_2(Phenylpropanoate)_4(H_2O)_2]$

The crystal structure of $Cu_2(phenylacetate)_4]\cdot 2H_2O$, **C3**, has been previously reported at 150 [27] and 298 [28] K. There are only slight differences in the cells' axis lengths and angles for these structures. We run the structure comparison tool available at the Bilbao Crystallographic Server [43] to compare the structure at 100 K reported in this article with the one obtained at room temperature, which presented the higher differences, finding a degree of lattice distortion of 0.0055 with a maximum difference of atomic positions of 0.1370 Å. **C3** also exhibits a paddle-wheel coordination motif with the carboxylate group in a bis-chelate fashion. In the case of **C1**, each carboxylate O atom coordinates to one copper(II) center. Meanwhile, in **C3**, an O atom from the carboxylate group can be connected to one or two copper(II) centers. This coordination motif gives rise to the formation of a 1D chain along the *a* axis.

In **C3**, the Cu···Cu distance is 2.5787(5) Å, also contained in the expected range. The same intermetal distance was observed in the structures with hexanoate [44], benzoate [45,46] and 2,3-dihydro-1,4-benzodioxine-6-carboxylate [47]. C-H···π interactions can be observed between phenyl rings of ligands within the paddle wheel on the 1D chain contiguous molecules with a centroid to H distance of 3.062 Å and an angle between the phenyl rings of 71.00°. The infinite chains are sustained with each other through dispersive interactions involving the phenyl groups. No obvious hydrogen bonds or π-stacking interactions can be observed in the structure.

The structure of $[Cu_2(phenylpropanoate)_4(H_2O)_2]$, **C2**, was also previously determined, showing a coordination scheme similar to that of **C3** [48]. In spite of that, according to the molecular formula found, it is possible that, in the compound prepared by us, the structure is similar to that of **C1**.

### 2.2. Infrared Spectra

The studied ternary complexes present similar infrared spectra. Table 3 presents a tentative assignment of the bands related to coordinating groups. In particular, the values of the Δν (calculated as $\nu(COO)_{as}$-$\nu(COO)_s$) for **C1** = 157 $cm^{-1}$, **C2** = 157 $cm^{-1}$ and **C3** = 176 $cm^{-1}$ agree with a bidentate coordination of the carboxylate [49], as observed in the crystal structures of **C1** and **C3**. The spectra of the complexes and the ligands are included in the supplementary material (Figures S2–S7).

**Table 3.** Wavenumber ($cm^{-1}$) of common bands in the complexes, and their tentative assignment.

| Compound | ν(O-H) | $\nu(C=O) + \nu(COO)_{as}$ | $\nu(COO)_s$ | ν(Cu-O) |
|---|---|---|---|---|
| $[Cu_2(3\text{-}(4\text{-hydroxyphenyl})propanoate)_4(H_2O)_2]\cdot 2H_2O$ | 3330 sh | 1582 s, 1516 w | 1425 m | 532 w |
| $[Cu_2(phenylpropanoate)_4(H_2O)_2]$ | 3500–3200 sh | 1588 s, 1516 w | 1431 m | 480 w |
| $[Cu_2(phenylacetate)_4]$ | 3500–3200 sh | 1594 s, 1514 s | 1438 m | 532 w |

### 2.3. Solution Studies

Major Species in Solution Characterization Using UV-Visible Spectra and Lipophilicity

The visible spectra of the complexes show an absorption band at around 710 nm (DMSO solution), as presented in Table 4, which, if compared with the wavelength of the maxima calculated according to the empiric correlation of Prenesti et al. [50,51], agrees with an equatorial coordination by four carboxylate oxygen atoms (calculated $\lambda_{max}$ 708 nm), as observed in the solid state. In relation to the dimeric structure, the occurrence of a band between 350 and 400 nm has been related to this species' existence in solution [52]. This band is present in the complexes' UV spectra but not in the ligand spectra. According to this analysis, in a DMSO solution, the complexes remain as dimers like the solid-state form of **C1**. The complexes are not soluble in $H_2O$, but, as an approach to studying their behavior in this solvent, spectra were also registered in a DMSO:water mixture (80:20), Table 4 presents the obtained results. The $\lambda_{max}$ shifts slightly, and the shape of the spectra-changed difference was accounted for by n ($n = \varepsilon_{850}/\varepsilon_{max} \times 100$), which is higher in an aqueous solution, suggesting a different degree of distortion of the coordination geometry depending on the solvent [53], as previously observed with other Cu complexes.

**Table 4.** Maximum absorption wavelength ($\lambda_{max}$, nm), molar absorptivity (ε, $M^{-1}cm^{-1}$) and n ($\varepsilon_{850}/\varepsilon_{max} \times 100$) of the spectra in DMSO and DMSO:$H_2O$ (80:20) and partition coefficients (P) between n-octanol and physiologic solution.

| Compound | λmax/ε * | n * | λmax/ε ** | n ** | P |
|---|---|---|---|---|---|
| $[Cu_2(3\text{-}(4\text{-hydroxyphenyl})propanoate)_4(H_2O)_2]\cdot 2H_2O$ | 710/388 | 43 | 726/134 | 65 | 0.10 |
| $[Cu_2(phenylpropanoate)_4(H_2O)_2]$ | 715/313 | 44 | 713/288 | 73 | 0.24 |
| $[Cu_2(phenylacetate)_4]$ | 711/404 | 48 | 736/150 | 72 | 0.47 |

* DMSO, ** DMSO:$H_2O$ (80:20), ε calculated per Cu mole.

The lipophilicity of the complexes is similar, with the hydroxyl group of **C1** giving rise to a slightly more hydrophilic compound, as expected.

### 2.4. Complex–DNA Binding Studies

#### 2.4.1. $K_b$ Determination (UV-Visible Spectra)

The intrinsic binding constants of the complexes to the DNA ($K_b$) were determined via UV-visible titration (Figure 2 and supplementary material Figures S8 and S9). Their values are presented in Table 5. The ligands produce nonappreciable DNA binding as studied via this technique.

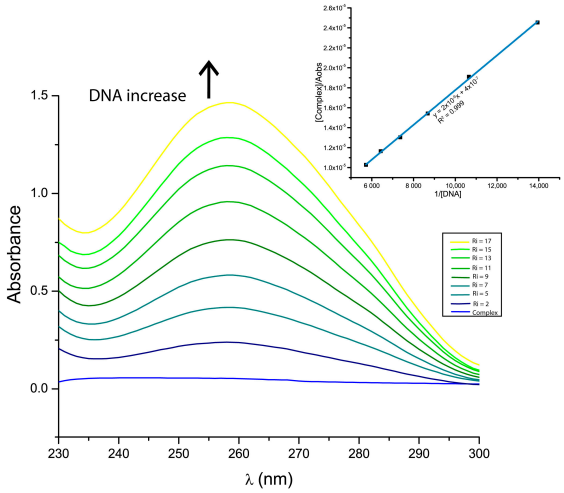


**Figure 2.** UV spectra of **C1** with increasing [DNA]/[complex] (*Ri*) ratio. Inset: [complex]/Aobs (i.e., the complex concentration/the measured absorbance) as a function of 1/[DNA] plot with regression parameters.

**Table 5.** DNA binding constants ($K_b$), as determined by the Benesi–Hildebrand method.

| Compound | C1 | C2 | C3 | L1 | L2 | L3 |
|---|---|---|---|---|---|---|
| $K_b$ (M-1) | $5.2 \times 10^2$ | $2.0 \times 10^2$ | $8.7 \times 10^2$ | ND * | ND * | ND * |

* Not Determined.

The observed values of $K_b$ are relatively low if compared with other Cu-carboxylate complexes. For instance, compounds $[Cu_2(nitrofenilacetate)_4)(H_2O)_2]$ and $[Cu_2(fenilbutanoate)_4]_n$ present $K_b$ values in the $10^3$–$10^4$ range [54,55]. In particular, the binding of **C3** on salmon sperm DNA was already reported and determined by the same methodology, with $K_b = 1.4 \times 10^4$ $M^{-1}$ nm on the used DNA being suggestive of intercalation in addition to binding by the grooves [27].

### 2.4.2. Mode of Binding (Relative Viscosity)

Relative viscosity is a highly sensitive method to detect changes in the overall length of the DNA caused by the interaction of small molecules [49]. Figure 3 presents the effect of the increasing concentration of the complexes on the relative viscosity of CT-DNA. Free ligands induce no appreciable change in DNA's relative viscosity, as detected by this technique. The complexes induce a slight relative viscosity decrease at the studied ratios. This suggests that the binding provokes bends in the DNA helix [56]. A small slope is observed, in agreement with the low $K_b$ of the complexes, evidencing that the binding event is relatively minor compared to other Cu complexes and induces only small changes in DNA conformation.

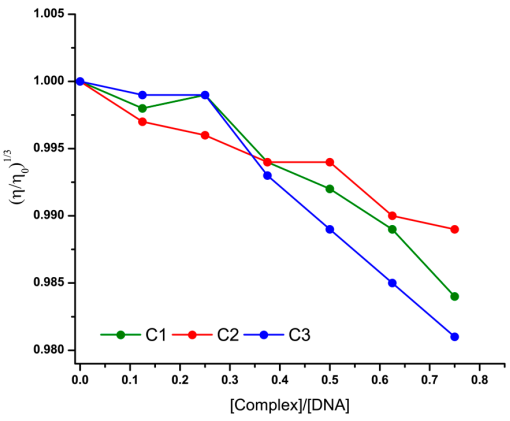


**Figure 3.** Effect of the increasing concentration of the complexes on the relative viscosity of CT-DNA.

### *2.5. Cytotoxicity of the Compounds*

The cytotoxicity of the complexes and free ligands was evaluated on four tumor and one nontumor cell lines; Table 6 presents the results expressed by $IC_{50}$. The ligands L1–L3 present no detectable cytotoxicity up to 100 μM.

**Table 6.** Cytotoxic activity (expressed by $IC_{50}$) of the studied complexes after 48 h of incubation, against MCF-7, MDA-MB-231 (human metastatic breast adenocarcinomas, the latter triple negative), A549 (human lung epithelial carcinoma), A278cis (human ovarian cisplatin-resistant) and MRC-5 (lung nontumoral) cell lines.

| | Cytotoxicity, IC50 (μM) | | | | |
|---|---|---|---|---|---|
| **Compound** | **MCF-7** | **MDA-MB-231** | **A549** | **A278cis** | **MRC-5** |
| **C1** | >50 | >50 | >50 | 26.80 ± 4.50 | >50 |
| **C2** | 20.20 ± 0.78 | >50 | >50 | 13.50 ± 0.57 | >50 |
| **C3** | >50 | >50 | >50 | 7.85 ± 0.86 | >50 |
| Cisplatin | 8.91 ± 2.60 | 24.90 ± 3.40 | 14.40 ± 1.40 | 26.90 ± 0.60 | 29.09 ± 0.78 |

The complexes induce low cytotoxicity to four of the studied lines but are cytotoxic to the A278cis cell line and resistant to cisplatin, therefore showing no cross resistance. This activity can be classified as moderate compared to other Cu complexes [3]. There seems to be a correlation between the $IC_{50}$ and lipophilicity (P). Both **C2** and **C3** are more cytotoxic than cisplatin on A278cis cells and are less toxic than cisplatin to the nontumor cell MRC-5, making both complexes **C2** and **C3** interesting complexes for further study of their activities on other tumor cells, especially those resistant to cisplatin.

## 3. Discussion

The compounds presented in this work are dimeric complexes in the solid state, with **C3** further extending into a polymeric structure. In a DMSO solution, the dimeric structure seems to be preserved. In the conditions of the biological assays, coordination may be altered, possibly including, in addition to carboxylate, other ligands such as residues from albumin. The biological activity of the compounds is different when compared with the free ligands, suggesting also that the ligands remain coordinated in the major species in these conditions.

The complexes bind the DNA with low $K_b$ compared to other Cu complexes; therefore, this seems not to be part of the mechanism of the cytotoxicity of the complexes.

This work aimed to find new complexes with interesting cytotoxic activity, particularly with ligands that present no appreciable toxicity. The complexes were active only in one of the studied tumor cells, a cell line that is resistant to cisplatin. This opens an opportunity to further explore the activity of **C2** and **C3** on other tumor cell lines. To date, there are few Cu(II) complexes that have ligands with low toxicity and are cytotoxic to tumor cells.

## 4. Materials and Methods

### *4.1. Synthetic Procedures*

All reagents were used as commercially available: copper(II) carbonate and copper(II) chloride (Fluka, SIGMA-Aldrich, St. Louis, MI, USA), carboxylic ligands (SIGMA-Aldrich, St. Louis, MI, USA) and calf thymus DNA (CT-DNA, SIGMA-Aldrich, St. Louis, MI, USA).

$[Cu_2(phenylcarboxylate)_4]$ Complexes

An ethanolic solution of phenylcarboxylate (0,23 mmol, 5 mL) was added under constant stirring at room temperature to an aqueous solution of copper(II) chloride (0,23 mmol, 5 mL). The solution turned green instantly. It was allowed to slowly evaporate giving rise to green prismatic single crystals adequate for X-ray diffraction studies. $[Cu_2(3\text{-}(4\text{-}hydroxyphenyl)propanoate)_4(H_2O)_2]\cdot 2H_2O$ (**C1**) Calc. for $C_{36}H_{44}Cu_2O_{12}$/Found: %C: 50.29/

50.15 %H: 5.16/5.45; [$Cu_2$(phenylpropanoate)$_4$($H_2O$)$_2$] (**C2**) Calc. for $C_{36}H_{40}Cu_2O_{10}$/Found: %C: 56.90/56.80 %H: 5.31/5.39; [$Cu_2$(phenylacetate)$_4$] (**C3**) Calc. for $C_{32}H_{28}Cu_2O_8$/Found: %C: 57.57/57.67 %H: 4.23/4.57.

### *4.2. Physical Methods*

#### 4.2.1. Characterization—General

Elemental analyses (C, N and H) of the samples were carried out on a Thermo Flash 2000 elemental analyzer (Thermo Fisher Scientific, USA). Infrared spectra were measured on a Shimadzu IR Prestige 21 (Shimadzu, Kyoto, Japan, 4000 to 400 $cm^{-1}$) as 1% KBr disks with a 4 $cm^{-1}$ resolution. UV-visible spectra of 5 mM solutions in DMSO or DMSO $H_2O$ (80:20) of the complexes were recorded on a ShimadzuUV1900 spectrophotometer (Shimadzu, Kyoto, Japan) in 1 cm path-length quartz cells.

#### 4.2.2. Crystal Structure Determination

Suitable single crystals of **C1** and **C3** were obtained from recrystallization from DMSO aqueous solution slow evaporation. Samples were mounted, and their diffraction patterns were measured on a Rigaku XtaLAB Synergy-S diffractometer (Rigaku, USA) equipped with an Oxford Cryosystems Cryostream 800 PLUS. The crystals were kept at a steady $T$ = 100(2) K during data collection with a PhotonJet (CuKα = 1.54184 Å) X-ray Source. CrysAlisPro v 42.84a software (Rigaku) was used to evaluate the collection strategy, data reduction and scaling, as well as absorption correction. The structure was solved using direct methods with ShelXt [57] and refined using the atoms in the molecules model with ShelXL-2019/2 [58] using least squares minimization on $F^2$. Both ShelXt and ShelXL were used within Olex2 [59]. Hydrogen atoms were geometrically positioned and refined isotopically with the riding model. Molecular graphics were prepared using Mercury [36].

The nonhydrogen atoms were refined anisotropically. Then, all hydrogen atoms were located from electron-density difference maps and were positioned geometrically and refined using the riding model [Uiso(H) = 1.2 Ueq or 1.5 Ueq]. The Olex2 was also used for analysis and visualization of the structures and for graphic material preparation. Table 1 summarizes the X-ray diffraction data and refinement parameters obtained for the elucidated crystal structures. The CIF files of complexes **C1** and **C3** were deposited in the Cambridge Structural Data Base under the CCDC numbers 2,288,430 and 2,288,436, respectively. Copies of the data can be obtained, free of charge, via www.ccdc.cam.ac.uk.

### *4.3. Lipophility Assessment*

Lipophilicity was studied by determining the partition coefficient of the complexes in n-octanol/physiological solution (0.9% NaCl in water). To 1 mL of n-octanol 0.2 mM solution of the complex, 1 mL of physiological solution was added. It was shaken for 1 h. Afterward, the samples were centrifugated, and the phases separated. UV-vis spectra were used to determine the concentration of the complex in each phase. The partition coefficient, P, was calculated as C n-octanol/Cwater.

### *4.4. DNA Interaction*

A stock solution of Calf Thymus DNA (CT-DNA, 5 mg in 5 mL $H_2O$) was prepared by stirring overnight, stored at 4 °C and used within 3 days. Its concentration was determined spectroscopically at 260 nm ($\varepsilon_{260}$ = 6600 $M^{-1}cm^{-1}$/base pair). The solution was free of protein, as determined by the $A_{260}/A_{280}$ ratio, which varied in the 1.8–1.9 range.

#### 4.4.1. DNA Binding Constant: UV Absorption Titration Experiments

The DNA intrinsic binding constant ($K_b$) was determined by UV absorption measurements using the Benesi–Hildebrand model [60,61]. Solutions of the complexes 5 mM, in buffer Tris/HCl pH = 7.5 and 50 mM in NaCl were used, and their concentration was kept

constant at 10–15 μM while adding CT-DNA to obtain concentrations in the 0–250 μM in the base pairs range. The Benesi–Hildebrand model can be described by the equation:

$$1/(\varepsilon a - \varepsilon f) = 1/(\varepsilon b - \varepsilon f) + 1/K_b[\text{DNA}]\ (\varepsilon b - \varepsilon f) \quad (1)$$

where [DNA] is the concentration of DNA, εa are the apparent absorption coefficients, εf and εb are the extinction coefficient for the free copper(II) complex and the extinction coefficient for the copper(II) complex in the fully bound form, respectively. In Equation (1), $1/(\varepsilon a - \varepsilon f)$ is equivalent to Aobserved/[Cu]. Therefore, according to this model, the $K_b$ value equals the slope to the intercept ratio of the plot [complex]/Aobserved as a function of 1/[DNA].

#### 4.4.2. DNA Binding Mode: Variation of Viscosity Experiments

Viscosity measurements were performed in an Ostwald-type viscosimeter (SIGMA-Aldrich, St. Louis, MI, USA) maintained at a temperature of 25.0 ± 0.1 °C in a thermostatic bath. Solutions of CT-DNA (150 μM base pairs) and complexes were prepared separately in Tris-HCl (5 mM, pH = 7.2, 50 mM NaCl) and thermostatized at 25 °C. Complex−DNA solutions (4 mL) were prepared just prior to running each experiment at different molar ratios ([complex]/[CT-DNA] = 0.125, 0.250, 0.375, 0.500, 0.625 and 0.750 (equivalent to [DNA]/[complex] ratio contained values of 8, 4, 2.7, 2 and 1.3). Solutions were equilibrated for 15 min at 25 °C, and, then, 5 flow times were registered. The relative viscosity of DNA in the absence ($\eta_0$) and presence (η) of complexes was calculated as $(\eta/\eta_0) = t - t_0/t_{DNA} - t_0$, where $t_0$ and $t_{DNA}$ are the flow times of the buffer and DNA solution, respectively, and t is the flow time of the DNA solution in the presence of copper complexes. Data are presented as a plot of $(\eta/\eta_0)^{1/3}$ versus the ratio of [complex]/[DNA [62].

### *4.5. Cytotoxicity Studies*

The cytotoxicity of the complexes was evaluated on human cancer cell lines: metastatic breast adenocarcinoma MDA-MB-231 (triple negative, ATCC: HTB-26), MCF-7 (ATCC: HTB-22), cisplatin-resistant ovarian carcinoma A2780cis (SIGMA), lung epithelial carcinoma A549 (ATCC: CCL-185) and on the nontumoral lung cell line MRC-5 (ATCC: CCL-171) using the MTT colorimetric assay. Cells were cultured in Dulbecco's Modified Eagle's Medium (DMEM) for MDA-MB-231, A549 and MRC-5, supplemented with 10% fetal bovine serum (FBS), Roswell Park Memorial Institute (RPMI) 1640 Medium for MCF-7 and A278cis, supplemented with 10% FBS, containing 1% penicillin and 1% streptomycin, at 310 K in a humidified 5% $CO_2$ atmosphere. In the assay, $1.5 \times 10^4$ cells/well were seeded in 150 μL of medium in 96-well plates and incubated at 310 K in 5% $CO_2$ for 24 h, to allow cell adhesion. Then cells were treated with copper complexes for 48 h. Cu complexes were dissolved in DMSO, and 0.75 μL of solution were added to each well with 150 μL of medium (final concentration of 0.5% DMSO/well). Cisplatin, used as a reference drug, was solubilized in DMF. Afterward, to detect cell viability, 3-(4,5-dimethylthiazol-2-yl)-2,5-diphenyltetrazolium bromide (MTT, 50 μL, 1 mg $mL^{-1}$ in PBS) was added to each well, and the plate was further incubated for 4 h. Living cells reduce MTT to purple formazan. The formazan crystals were solubilized with isopropanol (150 μL/well), and each well was measured with a microplate spectrophotometer at a wavelength of 540 nm. The concentration to 50% ($IC_{50}$) of cell viability (Table) was obtained from the analysis of absorbance data from three independent experiments.

**Supplementary Materials:** The following supporting information can be downloaded at: https://www.mdpi.com/article/10.3390/inorganics11100398/s1, Figure S1: Scheme of complexes. Figures S2–S7: Infrared spectra of complexes **C1**–**C3** and ligands L1–L3; Figures S8 and S9: UV spectra of **C2** (S7) and **C3** (S8) with increasing amounts of DNA. Inset: [complex]/Aobs as a function of 1/[DNA] plot with regression parameters.

**Author Contributions:** Conceptualization, G.F.; methodology, G.F. and A.A.B.; validation, G.F.; formal analysis, N.A. and J.E.; investigation, C.Y.F. and A.R.; resources, G.F.; data curation, C.Y.F.

and N.A.; writing—original draft preparation, G.F.; writing—review and editing, G.F., N.A., M.A., K.M., J.E., A.A.B. and A.J.C.-F.; visualization, N.A.; supervision, G.F.; project administration, G.F.; funding acquisition, C.Y.F., G.F.,M.A., A.J.C.-F., J.E. and A.A.B. All authors have read and agreed to the published version of the manuscript.

**Funding:** This research was funded by the Comisión Sectorial de Investigación Científica and Comisión Sectorial de Posgrado (CSIC and CAP respectively, UdelaR, CSIC I+D Grant to G. Facchin, CAP Grant to C.Y.F.), Programa de Desarrollo de las Ciencias Básicas (PEDECIBA Química) and Agencia Nacional de Investigación e Innovación (ANII), Uruguay and Fundação de Amparo à Pesquisa do Estado de São Paulo (FAPESP, Grant no. 2015/50366-7 and 2020/15542-7) and Conselho Nacional de Desenvolvimento Científico e Tecnológico (CNPq, Grants no 306682/2018-4 and 312505/2021-3), Brazil and Researchers Supporting Project number (RSP2023R147), King Saud University, Riyadh, Saudi Arabia.

**Data Availability Statement:** The data presented in this study are available in the article and Supplementary Material.

**Acknowledgments:** The authors acknowledge all the participant institutions. M.A. acknowledges the financial support through the Researchers Supporting Project number (RSP2023R147), King Saud University, Riyadh, Saudi Arabia.

**Conflicts of Interest:** The authors declare no conflict of interest.

## References

1. Romani, A.M.P. Cisplatin in cancer treatment. *Biochem. Pharmacol.* **2022**, *206*, 115323. [CrossRef]
2. Kellett, A.; Molphy, Z.; McKee, V.; Slator, C. Recent Advances in Anticancer Copper Compounds. In *Metal-Based Anticancer Agents*; Royal Society of Chemistry: London, UK, 2019; pp. 91–119.
3. Santini, C.; Pellei, M.; Gandin, V.; Porchia, M.; Tisato, F.; Marzano, C. Advances in Copper Complexes as Anticancer Agents. *Chem. Rev.* **2014**, *114*, 815–862. [CrossRef] [PubMed]
4. Zehra, S.; Tabassum, S.; Arjmand, F. Biochemical pathways of copper complexes: Progress over the past 5 years. *Drug Discov. Today* **2021**, *26*, 1086–1096. [CrossRef] [PubMed]
5. Krasnovskaya, O.; Naumov, A.; Guk, D.; Gorelkin, P.; Erofeev, A.; Beloglazkina, E.; Majouga, A. Copper Coordination Compounds as Biologically Active Agents. *Int. J. Mol. Sci.* **2020**, *21*, 3965. [CrossRef] [PubMed]
6. McGivern, T.; Afsharpour, S.; Marmion, C. Copper Complexes as Artificial DNA Metallonucleases: From Sigman's Reagent to Next Generation Anti-Cancer Agent? *Inorg. Chim. Acta* **2018**, *472*, 12–39. [CrossRef]
7. Shi, X.; Chen, Z.; Wang, Y.; Guo, Z.; Wang, X. Hypotoxic copper complexes with potent anti-metastatic and anti-angiogenic activities against cancer cells. *Dalton Trans.* **2018**, *47*, 5049–5054. [CrossRef] [PubMed]
8. Laws, K.; Suntharalingam, K. The next generation of anticancer metallopharmaceuticals: Cancer stem cell-active inorganics. *ChemBioChem* **2018**, *19*, 2246–2253. [CrossRef]
9. Kaur, P.; Johnson, A.; Northcote-Smith, J.; Lu, C.; Suntharalingam, K. Immunogenic Cell Death of Breast Cancer Stem Cells Induced by an Endoplasmic Reticulum-Targeting Copper(II) Complex. *ChemBioChem* **2020**, *21*, 3618–3624. [CrossRef]
10. Shi, X.; Fang, H.; Guo, Y.; Yuan, H.; Guo, Z.; Wang, X. Anticancer copper complex with nucleus, mitochondrion and cyclooxygenase-2 as multiple targets. *J. Inorg. Biochem.* **2019**, *190*, 38–44. [CrossRef]
11. Chang, M.R.; Rusanov, D.A.; Arakelyan, J.; Alshehri, M.; Asaturova, A.V.; Kireeva, G.S.; Babak, M.V.; Ang, W.H. Targeting emerging cancer hallmarks by transition metal complexes: Cancer stem cells and tumor microbiome. Part I. *Coord. Chem. Rev.* **2023**, *477*, 214923. [CrossRef]
12. Balsa, L.M.; Ruiz, M.C.; Santa Maria de la Parra, L.; Baran, E.J.; León, I.E. Anticancer and antimetastatic activity of copper(II)-tropolone complex against human breast cancer cells, breast multicellular spheroids and mammospheres. *J. Inorg. Biochem.* **2020**, *204*, 110975. [CrossRef] [PubMed]
13. da Silva, D.A.; De Luca, A.; Squitti, R.; Rongioletti, M.; Rossi, L.; Machado, C.M.L.; Cerchiaro, G. Copper in tumors and the use of copper-based compounds in cancer treatment. *J. Inorg. Biochem.* **2022**, *226*, 111634. [CrossRef] [PubMed]
14. Ruiz, M.C.; Perelmulter, K.; Levín, P.; Romo, A.I.B.; Lemus, L.; Fogolín, M.B.; León, I.E.; Di Virgilio, A.L. Antiproliferative activity of two copper (II) complexes on colorectal cancer cell models: Impact on ROS production, apoptosis induction and NF-κB inhibition. *Eur. J. Pharm. Sci.* **2022**, *169*, 106092. [CrossRef] [PubMed]
15. Figueroa-DePaz, Y.; Resendiz-Acevedo, K.; Davila-Manzanilla, S.G.; Garcia-Ramos, J.C.; Ortiz-Frade, L.; Serment-Guerrero, J.; Ruiz-Azuara, L. DNA, a target of mixed chelate copper(II) compounds (Casiopeinas(R)) studied by electrophoresis, UV-vis and circular dichroism techniques. *J. Inorg. Biochem.* **2022**, *231*, 111772. [CrossRef]
16. Peña, Q.; Sciortino, G.; Maréchal, J.-D.; Bertaina, S.; Simaan, A.J.; Lorenzo, J.; Capdevila, M.; Bayón, P.; Iranzo, O.; Palacios, Ò. Copper (II) N, N, O-Chelating Complexes as Potential Anticancer Agents. *Inorg. Chem.* **2021**, *60*, 2939–2952. [CrossRef]
17. Fernández, C.Y.; Alvarez, N.; Rocha, A.; Ellena, J.; Costa-Filho, A.J.; Batista, A.A.; Facchin, G. New Copper(II)-L-Dipeptide-Bathophenanthroline Complexes as Potential Anticancer Agents—Synthesis, Characterization and Cytotoxicity Studies—And Comparative DNA-Binding Study of Related Phen Complexes. *Molecules* **2023**, *28*, 896.

18. Alvarez, N.; Rocha, A.; Collazo, V.; Ellena, J.; Costa-Filho, A.J.; Batista, A.A.; Facchin, G. Development of Copper Complexes with Diimines and Dipicolinate as Anticancer Cytotoxic Agents. *Pharmaceutics* **2023**, *15*, 1345. [CrossRef]
19. Alvarez, N.; Leite, C.M.; Napoleone, A.; Mendes, L.F.S.; Fernandez, C.Y.; Ribeiro, R.R.; Ellena, J.; Batista, A.A.; Costa-Filho, A.J.; Facchin, G. Tetramethyl-phenanthroline copper complexes in the development of drugs to treat cancer: Synthesis, characterization and cytotoxicity studies of a series of copper(II)-L-dipeptide-3,4,7,8-tetramethyl-phenanthroline complexes. *J. Biol. Inorg. Chem.* **2022**, *27*, 431–441. [CrossRef]
20. Alvarez, N.; Viña, D.; Leite, C.M.; Mendes, L.F.; Batista, A.A.; Ellena, J.; Costa-Filho, A.J.; Facchin, G. Synthesis and structural characterization of a series of ternary copper (II)-L-dipeptide-neocuproine complexes. Study of their cytotoxicity against cancer cells including MDA-MB-231, triple negative breast cancer cells. *J. Inorg. Biochem.* **2020**, *203*, 110930. [CrossRef]
21. Alvarez, N.; Mendes, L.F.; Kramer, M.G.; Torre, M.H.; Costa-Filho, A.J.; Ellena, J.; Facchin, G. Development of Copper (II)-diimine-iminodiacetate mixed ligand complexes as potential antitumor agents. *Inorg. Chim. Acta* **2018**, *483*, 61–70. [CrossRef]
22. Alvarez, N.; Noble, C.; Torre, M.H.; Kremer, E.; Ellena, J.; Peres de Araujo, M.; Costa-Filho, A.J.; Mendes, L.F.; Kramer, M.G.; Facchin, G. Synthesis, structural characterization and cytotoxic activity against tumor cells of heteroleptic copper (I) complexes with aromatic diimines and phosphines. *Inorg. Chim. Acta* **2017**, *466*, 559–564. [CrossRef]
23. Iglesias, S.; Alvarez, N.; Kramer, G.; Torre, M.H.; Kremer, E.; Ellena, J.; Costa-Filho, A.J.; Facchin, G. Structural Characterization and Cytotoxic Activity of Heteroleptic Copper (II) Complexes with L-Dipeptides and 5-$NO_2$-Phenanthroline.: Crystal Structure of [Cu (Phe-Ala)(5-$NO_2$-Phen)]·4$H_2O$. *Struct. Chem. Crystallogr. Commun.* **2015**, *1*, 1–7.
24. Iglesias, S.; Alvarez, N.; Torre, M.H.; Kremer, E.; Ellena, J.; Ribeiro, R.R.; Barroso, R.P.; Costa-Filho, A.J.; Kramer, M.G.; Facchin, G. Synthesis, structural characterization and cytotoxic activity of ternary copper (II)–dipeptide–phenanthroline complexes. A step towards the development of new copper compounds for the treatment of cancer. *J. Inorg. Biochem.* **2014**, *139*, 117–123. [CrossRef] [PubMed]
25. Costa-Filho, A.J.; Nascimento, O.R.; Calvo, R. Electron paramagnetic resonance study of weak exchange interactions between metal ions in a model system: CuIIGly-Trp. *J. Phys. Chem. B* **2004**, *108*, 9549–9555. [CrossRef]
26. Balzano, T. Active Clinical Trials in Hepatic Encephalopathy: Something Old, Something New and Something Borrowed. *Neurochem. Res.* **2023**, *48*, 2309–2319. [CrossRef] [PubMed]
27. Iqbal, M.; Ali, S.; Tahir, M.N. Polymeric Copper(II) Paddlewheel Carboxylate: Structural Description, Electrochemistry, and DNA-binding Studies. *Z. Für Anorg. Und Allg. Chem.* **2018**, *644*, 172–179. [CrossRef]
28. Benslimane, M.; Redjel, Y.K.; Merazig, H.; Daran, J.-C. catena-Poly[bis([mu]3-2-phenylacetato-[kappa]3O,O′:O)bis([mu]2-2-phenylacetato-[kappa]2O:O′)dicopper(II)(Cu-Cu)]. *Acta Crystallogr. Sect. E* **2013**, *69*, m397. [CrossRef]
29. Rap, V.M.; Manohar, H. Synthesis and crystal structure of methanol and acetic acid adducts of copper acetate. Predominance of σ-interaction between the two copper atoms in the dimer. *Inorganica Chim. Acta* **1979**, *34*, L213–L214. [CrossRef]
30. Kanazawa, Y.; Mitsudome, T.; Takaya, H.; Hirano, M. Pd/Cu-Catalyzed Dehydrogenative Coupling of Dimethyl Phthalate: Synchrotron Radiation Sheds Light on the Cu Cycle Mechanism. *ACS Catal.* **2020**, *10*, 5909–5919. [CrossRef]
31. Kendin, M.; Nikiforov, A.; Svetogorov, R.; Degtyarenko, P.; Tsymbarenko, D. A 3D-Coordination Polymer Assembled from Copper Propionate Paddlewheels and Potassium Propionate 1D-Polymeric Rods Possessing a Temperature-Driven Single-Crystal-to-Single-Crystal Phase Transition. *Cryst. Growth Des.* **2021**, *21*, 6183–6194. [CrossRef]
32. Jassal, A.K.; Sharma, S.; Hundal, G.; Hundal, M.S. Structural Diversity, Thermal Studies, and Luminescent Properties of Metal Complexes of Dinitrobenzoates: A Single Crystal to Single Crystal Transformation from Dimeric to Polymeric Complex of Copper(II). *Cryst. Growth Des.* **2015**, *15*, 79–93. [CrossRef]
33. Udupa, M.R.; Krebs, B. Crystal and molecular structure of tetra-μ-N-acetylglycinatodiaquodicopper(II). *Inorganica Chim. Acta* **1979**, *37*, 1–4. [CrossRef]
34. Groom, C.R.; Bruno, I.J.; Lightfoot, M.P.; Ward, S.C. The Cambridge Structural Database. *Acta Crystallogr. Sect. B* **2016**, *72*, 171–179. [CrossRef] [PubMed]
35. Bruno, I.J.; Cole, J.C.; Edgington, P.R.; Kessler, M.; Macrae, C.F.; McCabe, P.; Pearson, J.; Taylor, R. New software for searching the Cambridge Structural Database and visualizing crystal structures. *Acta Crystallogr. Sect. B* **2002**, *58*, 389–397. [CrossRef]
36. Macrae, C.F.; Sovago, I.; Cottrell, S.J.; Galek, P.T.A.; McCabe, P.; Pidcock, E.; Platings, M.; Shields, G.P.; Stevens, J.S.; Towler, M.; et al. Mercury 4.0: From visualization to analysis, design and prediction. *J. Appl. Crystallogr.* **2020**, *53*, 226–235. [CrossRef]
37. Vaughan, G.B.M.; Schmidt, S.; Poulsen, H.F. Multicrystal approach to crystal structure solution and refinement. *Z. Für Krist. Cryst. Mater.* **2004**, *219*, 813–825. [CrossRef]
38. Wang, Y.Y.; Shi, Q.; Shi, Q.Z.; Gao, Y.C. Self-assembly of porous two-dimensional copper(II) α, β-unsaturated carboxylate complexes with trimethyl phosphate. *Transit. Met. Chem.* **2000**, *25*, 382–387. [CrossRef]
39. Pathak, S.; Biswas, N.; Jana, B.; Ghorai, T.K. Synthesis and characterization of a nano Cu2 cluster. *Adv. Mater. Proc.* **2017**, *2*, 275–279.
40. Li, J.-R.; Yu, J.; Lu, W.; Sun, L.-B.; Sculley, J.; Balbuena, P.B.; Zhou, H.-C. Porous materials with pre-designed single-molecule traps for CO2 selective adsorption. *Nat. Commun.* **2013**, *4*, 1538. [CrossRef]
41. Kristiansson, O.; Tergenius, L.-E. Structure and host–guest properties of the nanoporous diaquatetrakis(p-nitrobenzoato)dicopper(II) framework. *J. Chem. Soc. Dalton Trans.* **2001**, *9*, 1415–1420. [CrossRef]
42. Desiraju, G.R. A Bond by Any Other Name. *Angew. Chem. Int. Ed.* **2011**, *50*, 52–59. [CrossRef] [PubMed]
43. de la Flor, G.; Orobengoa, D.; Tasci, E.; Perez-Mato, J.M.; Aroyo, M.I. Comparison of structures applying the tools available at the Bilbao Crystallographic Server. *J. Appl. Crystallogr.* **2016**, *49*, 653–664. [CrossRef]

44. Doyle, A.; Felcman, J.; Gambardella, M.T.d.P.; Verani, C.N.; Tristão, M.L.B. Anhydrous copper(II) hexanoate from cuprous and cupric oxides. The crystal and molecular structure of $Cu_2(O_2CC_5H_{11})_4$. *Polyhedron* **2000**, *19*, 2621–2627. [CrossRef]
45. Katzsch, F.; Münch, A.S.; Mertens, F.O.R.L.; Weber, E. Copper(II) benzoate dimers coordinated by different linear alcohols—A systematic study of crystal structures. *J. Mol. Struct.* **2014**, *1064*, 122–129. [CrossRef]
46. Krause, L.; Herbst-Irmer, R.; Stalke, D. An empirical correction for the influence of low-energy contamination. *J. Appl. Crystallogr.* **2015**, *48*, 1907–1913. [CrossRef]
47. Sheng, G.-H.; Zhou, Q.-C.; Sun, J.; Cheng, X.-S.; Qian, S.-S.; Zhang, C.-Y.; You, Z.-L.; Zhu, H.-L. Synthesis, structure, and urease inhibitory activities of three binuclear copper(II) complexes with protocatechuic acid derivative. *J. Coord. Chem.* **2014**, *67*, 1265–1278. [CrossRef]
48. Massignani, S.; Scatena, R.; Lanza, A.; Monari, M.; Condello, F.; Nestola, F.; Pettinari, C.; Zorzi, F.; Pandolfo, L. Coordination polymers from mild condition reactions of copper(II) carboxylates with pyrazole (Hpz). Influence of carboxylate basicity on the self-assembly of the $[Cu_3(\mu_3\text{-OH})(\mu\text{-pz})_3]^{2+}$ secondary building unit. *Inorg. Chim. Acta* **2017**, *455*, 618–626. [CrossRef]
49. Nakamoto, K. *Infrared and Raman Spectra of Inorganic and Coordination Compounds, Applications in Coordination, Organometallic, and Bioinorganic Chemistry*, 6th ed.; Wiley-Interscience: Hoboken, NJ, USA, 2009.
50. Prenesti, E.; Daniele, P.; Prencipe, M.; Ostacoli, G. Spectrum–structure correlation for visible absorption spectra of copper (II) complexes in aqueous solution. *Polyhedron* **1999**, *18*, 3233–3241. [CrossRef]
51. Prenesti, E.; Daniele, P.G.; Berto, S.; Toso, S. Spectrum–structure correlation for visible absorption spectra of copper (II) complexes showing axial co-ordination in aqueous solution. *Polyhedron* **2006**, *25*, 2815–2823. [CrossRef]
52. Karaliota, A.; Kretsi, O.; Tzougraki, C. Synthesis and characterization of a binuclear coumarin-3-carboxylate copper(II) complex. *J. Inorg. Biochem.* **2001**, *84*, 33–37. [CrossRef]
53. Bhirud, R.G.; Srivastava, T.S. Synthesis, characterization and superoxide dismutase activity of some ternary copper (II) dipeptide-2, 2′-bipyridine, 1, 10-phenanthroline and 2, 9-dimethyl-1, 10-phenanthroline complexes. *Inorg. Chim. Acta* **1991**, *179*, 125–131. [CrossRef]
54. Muhammad, N.; Ikram, M.; Perveen, F.; Ibrahim, M.; Ibrahim, M.; Abel; Viola; Rehman, S.; Shujah, S.; Khan, W.; et al. Syntheses, crystal structures and DNA binding potential of copper(II) carboxylates. *J. Mol. Struct.* **2019**, *1196*, 771–782. [CrossRef]
55. Iqbal, M.; Ali, S.; Tahir, M.N.; Haleem, M.A.; Gulab, H.; Shah, N.A. A binary copper(II) complex having a stepped polymeric structure: Synthesis, characterization, DNA-binding and anti-fungal studies. *J. Serb. Chem. Soc.* **2020**, *85*, 203–214. [CrossRef]
56. Suh, D.; Chaires, J.B. Criteria for the mode of binding of DNA binding agents. *Bioorg. Med. Chem.* **1995**, *3*, 723–728. [CrossRef]
57. Sheldrick, G. SHELXT—Integrated space-group and crystal-structure determination. *Acta Crystallogr. Sect. A* **2015**, *71*, 3–8. [CrossRef]
58. Sheldrick, G. Crystal structure refinement with SHELXL. *Acta Crystallogr. Sect. C* **2015**, *71*, 3–8. [CrossRef] [PubMed]
59. Dolomanov, O.V.; Bourhis, L.J.; Gildea, R.J.; Howard, J.A.K.; Puschmann, H. OLEX2: A complete structure solution, refinement and analysis program. *J. Appl. Crystallogr.* **2009**, *42*, 339–341. [CrossRef]
60. Benesi, H.A.; Hildebrand, J.H. A Spectrophotometric Investigation of the Interaction of Iodine with Aromatic Hydrocarbons. *J. Am. Chem. Soc.* **2002**, *71*, 2703–2707. [CrossRef]
61. Sirajuddin, M.; Ali, S.; Badshah, A. DRUG-DNA Interactions and their study by UV-visible, fluorescence spectroscopies and cyclic voltametry. *J. Photochem. Photobiol. B Biol.* **2013**, *124*, 1–19. [CrossRef]
62. Scruggs, R.L.; Ross, P.D. Viscosity study of DNA. *Biopolymers* **1964**, *2*, 593–609. [CrossRef]


**Disclaimer/Publisher's Note:** The statements, opinions and data contained in all publications are solely those of the individual author(s) and contributor(s) and not of MDPI and/or the editor(s). MDPI and/or the editor(s) disclaim responsibility for any injury to people or property resulting from any ideas, methods, instructions or products referred to in the content.